IIETA International Information and Engineering Technology Association
Advancing the World of Information and Engineering

Journal of New Materials for Electrochemical Systems
Vol.22, No.4, October, 2019, pp. 191-194
http://new-mat.org
http://iieta.org/journals/jnmes

Evaluations of Discharge Capacity and Cycle Stability on Graphene-added $Li_{1.9}Ni_{0.35}Mn_{0.65}O_2$ Cathode by Carbonate Co-precipitation

Seon-Jin Lee[1], Seong-Jae Kim[2] and Tae-Whan Hong[3,*]

[1]Department of Nano-Polymer Science & Engineering, Korea National University of Transportation, Chungju, Chungbuk 380-702, Republic of Korea
[2]Departmeent of Mechanical Engineering, Dong-A University, Busan 49315, Republic of Korea
[3]Department of advanced Materials Engineering, Korea National University of Transportation, Chungju, Chungbuk 380-702, Republic of Korea

Corresponding Author Email: twhong@ut.ac.kr

ABSTRACT

$Li[Li_{1/3-2x/3}Ni_xMn_{2/3-x/3}]O_2$ is currently receiving considerable attention for its use as a modern cathode material for lithium-ion batteries (LIBs), owing to its high capacity of over 250 $mAhg^{-1}$ when charged to 4.5 V or higher. However, owing to the rapidly fading capacity and poor rate capability of $Li[Li_{1/3-2x/3}Ni_xMn_{2/3-x/3}]O_2$ materials, extensive efforts have been made in recent years to improve their rate capability. In this paper, a Li-rich and manganese-based $Li_{1.9}Ni_{0.35}Mn_{0.65}O_2$ cathode material was prepared by a carbonate co-precipitation method, and graphene, which provides high conductivity and thermal stability, was used during the slurry mixing process. X-ray diffraction (XRD) and scanning electron microscopy (SEM) were used to characterize their structure and microstructure. The electrochemical properties show that the initial discharge capacity and cycle stability were enhanced due to the high electrical conductivity and thermal stability of graphene.

PACS number: 73.20.At

Keywords: *Mn-rich cathode, Carbonate co-precipitation, Graphene*

Received: December-21-2018, Accepted: April-01-2019, https://doi.org/10.14447/jnmes.v22i4.a04

I. INTRODUCTION

High energy and power-density lithium-ion batteries (LIBs) are critically needed for both vehicle and stationary storage applications [1,2]. Unfortunately, the current lithium-ion cathode material does not meet the demands for higher energy and power densities [3,4]. Searching for cheaper and safer cathode materials with higher capacity has become a significant subject of research. In this regard, the Li-rich and manganese-based layered solid-solution between layered $LiMO_2$ (M = Ni, Co, and Mn) and layered $Li[Li_{1/3}Mn_{2/3}]O_2$ (commonly designated as Li_2MnO_3) have become attractive cathode materials owing to their high capacity (>250 mAh g^{-1}), low cost, and enhanced structural stability [5-7] compared to the commercially available cathodes. Unfortunately, these complicated materials are difficult to prepare and they could show low rate capability depending on the synthetic route.

The co-precipitation method [8,9] is an efficient way to produce the current cathode materials, and most of the precursors are synthesized as transition metal hydroxides [10-13]. However, the hydroxide co-precipitation method is not easily controlled for the manganese-rich materials because $Mn(OH)_2$ easily oxidizes to the MnOOH and/or Mn_3O_4 phases during or after the co-precipitation process, leading to a deviation from the desired stoichiometry, impurities, and low tap density. To solve this problem, a carbonate co-precipitation method [14-16] is suitable to synthesize the transition metal (Ni, Co, Mn) precursors. In principle, the carbonate co-precipitation method has the advantage of maintaining the constant oxidation states of Ni, Co, and Mn (equal to 2) in the carbonate matrix [17]. In addition, the experimental conditions of carbonate co-precipitation are less harsh than those of the hydroxide co-precipitation, such as the easy control of the pH value and no need for an inert atmosphere.

Although Li-rich materials have a big advantage over current commercial cathode materials with their higher capacity, their low conductivities are considered to be their main drawback, limiting their rate capability and, to some extent, cyclability. There have been numerous attempts to improve Li-rich materials' rate capability by modifying the grain shape and size, doping, and adding electrically conductive additives [18-22]. As shown further, some experimental works with graphene oxide or reduced graphene oxide (rGO) as the conductive additive offer a superior rate capability to those achieved by other methods. However, it is very rare to apply graphene alone to Mn-rich cathode materials prepared by the carbonate co-precipitation method. In this paper, we report the addition of graphene to $Li_{1.9}Ni_{0.35}Mn_{0.65}O_2$ (LMNO), synthesized by carbonate co-precipitation.

2. EXPERIMENTAL

2.1. Synthesis of $Li_{1.9}Ni_{0.35}Co_{0.65}Mn_{0.1}O_2$

$[Ni_{0.35}Mn_{0.65}]CO_3$ powders were prepared by co-precipitation, as previously reported. An aqueous solution of $NiSO_4$ $6H_2O$ and $MnSO_4 \cdot H_2O$ was pumped into a continuously stirred tank reactor in an N2 atmosphere. Simultaneously, a Na_2CO_3 solution and an appropriate amount of NH_4OH solution (chelating agent) were fed separately into the reactor. The spherical $[Ni_{0.35}Mn_{0.65}]CO_3$ powders were dried at 130°C for 24 h to remove adsorbed water. Finally, $[Ni_{0.35}Mn_{0.65}]CO_3$, $LiOH \cdot H_2O$ was mixed at room temperature for 1 h, then calcined at 950°C for 24 h in air. The obtained $[Ni_{0.35}Mn_{0.65}]CO_3$ precursor was thoroughly mixed with an appropriate amount of Li_2CO_3 and calcined at 950°C for 24 hrs in air.

2.2. Material characterization

The XRD patterns for the cathodes were obtained using a Siemens D-5000 diffractometer in the 2θ range from 10° to 80° with Cu Kα

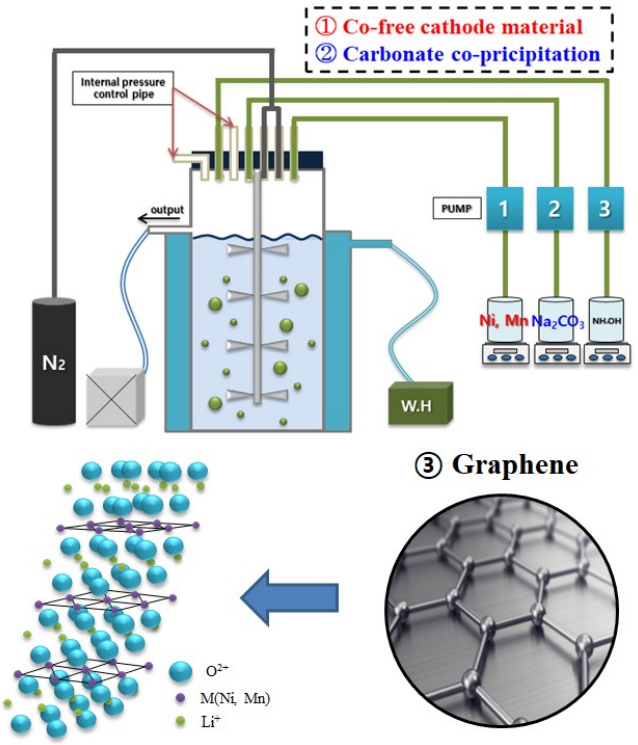

Fig. 1. Illustration of the strategy of this study.

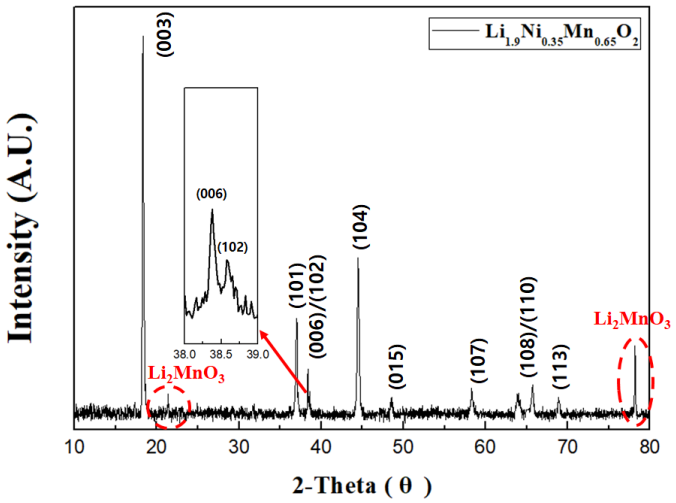

Fig. 2. XRD patterns of the $Li_{1.9}Ni_{0.35}Mn_{0.65}O_2$

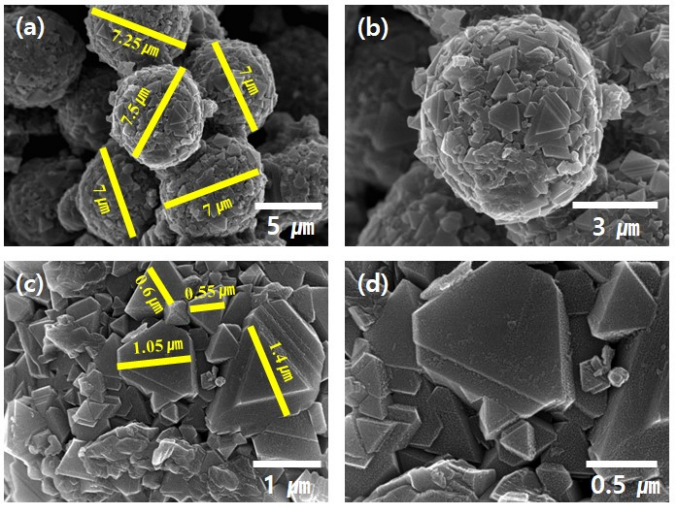

Fig. 3. SEM images of the $Li_{1.9}Ni_{0.35}Mn_{0.65}O_2$ particles: (a) X 5000, (b) X 10,000, (c) X 25,000, (d) X 50,000.

radiation (λ = 1.54068 Å). The morphology of the obtained powder was observed with SEM (JSM-7610F, JEOL).

2.3. Process of adding graphene and electrochemical test

To prepare the positive electrode, 80% $Li_{1.9}Ni_{0.35}Mn_{0.65}O_2$ powder 10 % super-P carbon black (Aldrich), N-methyl-2-pyrrolidone, 10% PVDF (Kureha KF100) binder, and 1 wt% graphene (electrical conductivity > 10^3 S/cm, Aldrich) versus the cathode were added to a crucible. After grinding, the viscous slurry was coated on aluminum foil using a doctor blade to make a film with a uniform thickness. The film was then dried at 120°C for 4 h in a vacuum oven. The CR2032-type coin cell was assembled in a glovebox using the above cathode film, lithium, a porous polypropylene film, and a 1M LiPF6 solution with a 3:7 volume ratio of ethylene carbonate (EC)/dimethyl carbonate (DMC). The lithium metal foil was used as both the counter and reference electrode. After the coin cell assembly, the test cells were charged and discharged galvano-statically between 2.0 and 4.8 V versus the Li/Li+, at a constant current density (17 mAg^{-1} was assumed to be 0.1 C rate). The cycle performances were carried out at a high current density (170 mAg^{-1} was assumed to be 1 C rate).

3. RESULTS AND DISCUSSION

Figure 1 shows an image of the strategy of this study; 1. Production of Co-free $Li_{1.9}Ni_{0.35}Mn_{0.65}O_2$ cathode materials of cheaper, safer, and higher capacity. 2. Suppression of MnOOH and Mn_3O_4 formation by carbonate co-precipitation, and 3. Enhancement of electrical conductivity and thermal stability of cathode materials using graphene.

The XRD patterns of LMNO are shown in Fig. 2. As can be seen, $Li_{1.9}Ni_{0.35}Mn_{0.65}O_2$ exhibits layered characteristics and all peaks can be indexed to the hexagonal α-$NaFeO_2$ structure (space group: R3m, No. 166), except for two peaks (red dashed circles). These peaks may have been caused by Li_2MnO_3. Except for Li_2MnO_3, the peaks are very sharp, which indicate good crystallinity of the as-prepared materials. In addition, the separations between the adjacent peaks of (006)/(012) and (018)/(110) can be clearly observed, indicating a typical layered structure.

Figure 3 shows the SEM images of the $Li_{1.9}Ni_{0.35}Mn_{0.65}O_2$ powder. The estimated average particle size was 7 to 8 μm, and the secondary particles had a spherical morphology, as shown in Figs. 3 (a) and (b). The primary particles of $Li_{1.9}Ni_{0.35}Mn_{0.65}O_2$ were like a triangular prism in shape, with a particle size of 1.4 to 0.55 nm, as shown in Figs. 3 (c) and (d), and they were densely agglomerated, producing secondary forms.

The initial charge/discharge curves for the pristine and graphene-added LMNO cells with a constant current density of 17 mA/g (0.1C) cycled in the voltage range of 2.0 and 4.8 V are shown in Fig. 4. As predicted in Fig. 2, a high ratio of the electrochemically inactive Li_2MnO_3 plateau was clearly observed in the initial charge curve at all samples, as shown Fig. 4 (a). The dQ/dV plots show that the exact amount

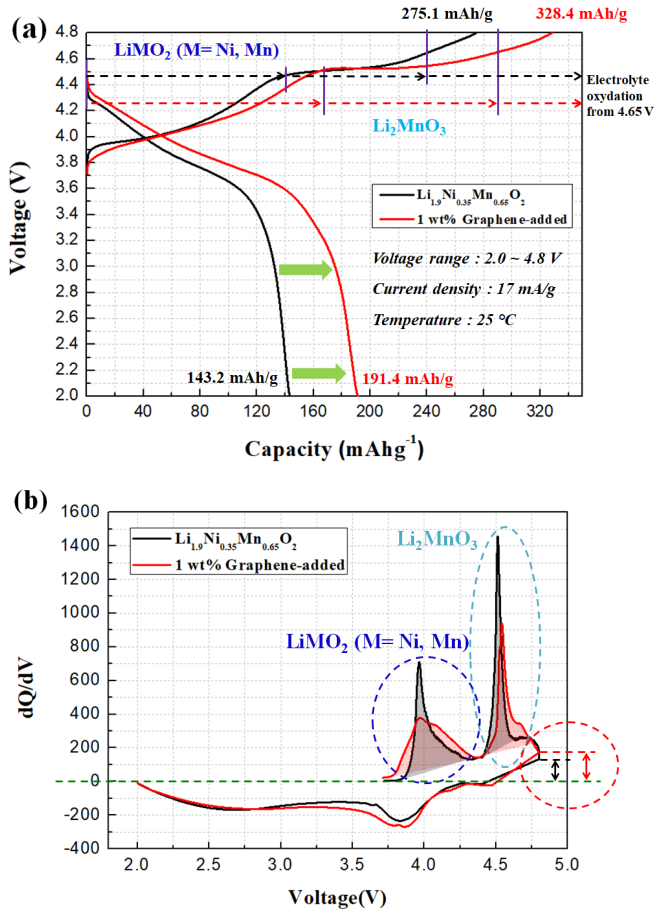

Fig. 4. (a) The initial charge/discharge curves and (b) the corresponding dQ/dV plots of the pristine and graphene-added $Li_{1.9}Ni_{0.35}Mn_{0.65}O_2$ at 0.1 C between 2.0 V and 4.8 V at 25°C.

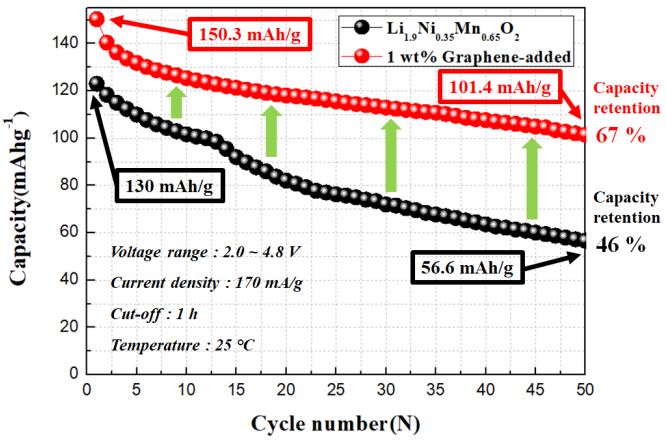

Fig. 5. Cyclic performances of the pristine and graphene-added $Li_{1.9}Ni_{0.35}Mn_{0.65}O_2$ at 1 C between 2.0 V and 4.8 V at 25°C.

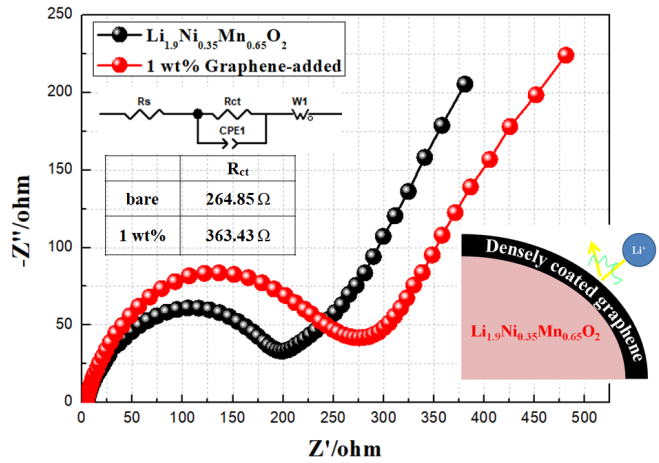

Fig. 6. Impedance plots of the pristine and graphene-added $Li_{1.9}Ni_{0.35}Mn_{0.65}O_2$.

of Li_2MO_3 and $LiMO_2$ can be calculated through integration, as shown Fig. 4 (b). Interestingly, as shown Fig. 4 (b), both samples failed to extract all lithium even at a high voltage of 4.8 V. Despite the high electrical conductivity of the graphene, the graphene-added sample caused less delithiation. This phenomenon is evidence that there was interference with the delithiation. Therefore, it is necessary to confirm this phenomenon through an additional impedance measurement. The initial discharge capacities of the pristine and graphene-added LMNO were 143.2 mAh/g and 191.4 mAh/g, respectively. This enhanced capacity is due to the high electrical conductivity of graphene. In addition, with graphene, the columbic efficient LMNO increased from 52% to 58%. All cells first had an irreversible capacity, of which the voltage plateau was due to the extraction of lithium and oxygen starting at approximately 4.4V, and their columbic efficiency stabilized after the second cycling [23]. The irreversible capacity of all samples probably resulted from the oxygen loss from the structure during first cycling as well as the possible electrolyte decomposition, since the onset potential of the electrolyte is approximately 4.65 V, depending on electrolyte composition [24]. Some portion of the irreversible capacity for all samples in Fig. 4 may come from the electrolyte oxidation. The most irreversible capacity may be related to the oxygen loss when the cell was charged above 4.45 V [24]. Therefore, the enhanced columbic efficient is due to the high thermal stability of graphene at the high working voltage.

Figure 5 shows the cycle performance of the pristine and graphene-added LMNO electrodes at a current density of 170 mA/g (1 C) from 2.0 V to 4.8 V. The initial discharge capacity of the pristine electrode increased from 123 $mAhg^{-1}$ to 56.6 $mAhg^{-1}$ by the 50th cycle (50th cycle efficiency = 46%). The graphene-added LMNO electrode delivered an initial discharge capacity of 150.3 $mAhg^{-1}$, which decreased to 101.4 $mAhg^{-1}$ after the 50th cycle (50th cycle efficiency = 67%). As can be seen in Fig. 5, the sample with graphene was found to be more stable than the pristine as the cycle progressed.

Figure 6 shows the electrochemical impedance spectra for the pristine and graphene-added LMNO materials after 1 cycle. Although the graphene had been added, the charge-transfer resistance (R_{ct}) values for these cathode materials increased from 264.8 Ω to 363.4 Ω. This result was predicted due to the increase in electrochemically inactive Li_2MnO_3, as shown in Fig. 4b (sky color dashed circle). In addition, one plausible reason for this is due to the densely coated graphene-blocking lithium ions, as shown in Fig. 4b (red dashed circle).

4. CONCLUSIONS

$Li_{1.9}Ni_{0.35}Mn_{0.65}O_2$ cathode material was prepared by a carbonate co-precipitation method and graphene was used during the slurry mixing process. The XRD results indicated a well indexed α-$NaFeO_2$ structure.

However, the peak intensity of Li_2MnO_3 was slightly larger. The SEM images showed that the $Li_{1.9}Ni_{0.35}Mn_{0.65}O_2$ cathode material size ranged from 7 μm to 8 μm, and the primary particles were triangular-prism-like in shape. The initial discharge capacities of the pristine and graphene-added $Li_{1.9}Ni_{0.35}Mn_{0.65}O_2$ were 143.2 mAh/g and 191.4 mAh/g, respectively. The cycle performances of the pristine and graphene-added LMNO electrodes were evaluated at a current density of 170 mA/g (1 C) from 2.0 V to 4.8 V at room temperature. The capacity retention of the pristine and graphene-added $Li_{1.9}Ni_{0.35}Mn_{0.65}O_2$ were 46% to 67% after the 50^{th} cycle, respectively. The graphene-added $Li_{1.9}Ni_{0.35}Mn_{0.65}O_2$ had a significantly improved capacity and cycling stability due to the enhanced electrical conductivity and thermal stability.

5. ACKNOWLEDGMENTS

This study was supported by a grant from the Ministry of Trade Industry and Energy of the Republic of Korea (G02N03620000901).

REFERENCES

[1] M. Armand, J.-M.Tarascon, Nature, 451, 652 (2008).
[2] B. Dunn, H. Kamath, J.-M.Tarascon, Science, 334, 928 (2011).
[3] P.G. Bruce, S.A. Freunberger, L.J. Hardwick, J.M. Tarascon, Nat. Mater., 11, 19 (2011).
[4] M.M. Thackeray, C. Wolverton, E.D. Isaacs, Energy Environ. Sci., 5, 7854 (2012).
[5] J.-H. Kim, C.S. Yoon, Y.-K. Sun, J. Electrochem. Soc., 150, 538 (2003).
[6] C.S. Johnson, J.-S. Kim, C. Lefief, N. Li, J.T. Vaughey, M.M. Thackeray, Electrochem. Commun., 6, 1085 (2004).
[7] T.A. Arunkumar, E. Alvarez, A. Manthiram, J. Electrochem. Soc., 154, 770 (2007).
[8] M.E. Spahr, P. Novak, B. Schnyder, O. Haas, R. Nesper, J. Electrochem. Soc., 145, 1113 (1998).
[9] C. Storey, I. Kargina, Y. Grincourt, I.J. Davidson, Y.C. Yoo, D.Y. Seung, J. Power Sources, 97-98, 541 (2001).
[10]M.M. Thackeray, S.-H. Kang, C.S. Johnson, J.T. Vaughey, S.A. Hackney, Electrochem. Commun., 8, 1531 (2006).
[11]Y. Chen, G.F. Xu, J.L. Li, Y.K. Zhang, Z. Chen, F.Y. Kang, Electrochim. Acta, 87, 686 (2013).
[12]M.-H. Lee, Y.-J.Kang, S.-T.Myung, Y.-K. Sun, Electrochim. Acta, 50, 939 (2004).
[13]C.S. Johnson, J.-S. Kim, A.J. Kropf, A.J. Kahaian, J.T. Vaughey, L.M.L. Fransson, K. Edstrom, M.M. Thackeray, Chem. Mater., 15, 2313 (2003).
[14] X.Q. Liu, Z.M. Guo, Prog. Nat. Sci. Mater. Int., 22, 126 (2012).
[15]J.W. Zhang, X. Guo, S.M. Yao, W.T. Zhu, X.P. Qiu, J. Power Sources, 238, 245 (2013).
[16]M. Gao, F. Lian, H.Q. Liu, C.J. Tian, L.L. Ma, W.Y. Yang, Electrochim. Acta, 95, 87 (2013).
[17]S.-H. Park, S.-H. Kang, I. Belharouak, Y.K. Sun, K. Amine, J. Power Sources, 177, 177 (2008).
[18]M. Konarova, I. Taniguchi, J. Power Sources, 195, 3661 (2010).
[19]Y. Ge, X. Yan, J. Liu, X. Zhang, J. Wang, X. He, R. Wang, H. Xie, Electrochim. Acta, 55, 5886 (2010).
[20]Y. Yang, X.-Z.Liao, Z.-F.Ma, B.-F. Wang, L. He, Y.-S.He, Electrochem. Commun., 11, 1277 (2009).
[21]X. Li, F. Kang, X. Bai, W. Shen, Electrochem. Commun., 9, 663 (2007).
[22]B. Huang, X. Zheng, D. Jia, M. Lu, Electrochim. Acta, 55, 1227 (2010).
[23]D.-K.Lee, S.-H.Park, K.Amine, H.J.Bang, J.Parakash, Y.-K.Sun J. Power Sources, 162, 1346 (2009).
[24]Z. Lu, J.R. Dahn, J. Electrochem. Soc., 149, 815 (2002).